Journal of Environmental Management 154 (2015) 216–224

Contents lists available at ScienceDirect

Journal of Environmental Management

journal homepage: www.elsevier.com/locate/jenvman

Evaluation of an adsorption system to concentrate VOC in air streams prior to catalytic incineration

María A. Campesi [a, b], Carlos D. Luzi [a, b], Guillermo F. Barreto [a, b], Osvaldo M. Martínez [a, b, *]

[a] Departamento de Ingeniería Química, Facultad de Ingeniería, Universidad Nacional de La Plata (UNLP) 1 y 47, CP 1900 La Plata, Argentina
[b] CINDECA, CCT La Plata (CONICET-UNLP), Calle 47 N° 257, CP B1900AJK La Plata, Argentina

ARTICLE INFO

Article history:
Received 18 December 2014
Received in revised form
13 February 2015
Accepted 14 February 2015
Available online

Keywords:
VOC concentration
Thermal swing adsorption
Catalytic incineration
Rotor concentrator
Activated carbon

ABSTRACT

Catalytic combustion is a well-developed process for the removal of volatile organic compounds (VOCs). In order to reduce both the amount of catalyst needed for incineration and the surface area of recuperative heat exchangers, an evaluation of the use of thermal swing adsorption as a previous step for VOC concentration is made. An air stream containing ethyl acetate and ethanol (employed as solvents in printing processes) has been taken as a case study. Based on the characteristics of the adsorption/desorption system and the properties of the stream to be treated, a monolithic rotor concentrator with activated carbon as adsorbent material is adopted. Once the temperature of the inlet desorption stream T_D is chosen, the minimum possible desorption flow rate, $W_{D,min}$, and the amount of adsorbent material can be properly defined according to the extent of the Mass Transfer Zone (MTZ) at the end of the adsorption stage. An approximate procedure to speed up the calculations needed for sizing the bed and predicting the operating variables is also presented. In the case studied here, the concentration of the VOC stream can reach 6 times that of the primary effluent when $T_D = 200$ °C is chosen.

1. Introduction

The growth of industrial production is one of the main reasons for the significant increase in air pollution. As part of this problem, Volatile Organic Compounds (VOCs) are an important type of air pollutants.

Technologies for removing VOCs from effluents (mainly air) are classified as either destructive or recuperative. The specific purpose and/or the economic analysis of the treatment are key factors when choosing the best alternative (Khan and Goshal, 2000). Catalytic oxidation is the most widespread option among destructive alternatives. The use of a catalyst allows for the use of much lower operating temperatures than thermal oxidation. However, current catalytic materials require temperatures well above ambient levels (Everaert and Baeyens, 2004). Typical values are usually higher than around 200 °C (Delimaris and Ioannides, 2009; Santos et al., 2011; Campesi et al., 2012a), although the precise temperature depends on the type of VOC. Very often high flow rates of VOC-laden air stream at nearly ambient temperature have to be treated, typically between 5 and 50 Nm^3/s. Consequently, catalytic oxidation needs bulky catalyst beds and preheating of the incoming effluent with the clean exit stream requires a large exchange surface area, due to the high flow rates and the low thermal driving force. The latter is essentially set by the adiabatic temperature rise, ΔT_{ad}, in the reactor.

Concentration of VOCs by including a thermal swing adsorption cycle (Yang, 1997) as a previous step to catalytic incineration (Sramek et al., 2004; Nikolajsen et al., 2006; Yamaguchi et al., 2013), is an alternative method for a significant reduction in the size of the catalyst bed and heat exchangers. A typical combined system is shown in Fig. 1. The main components are the adsorption/desorption device, the adiabatic catalytic reactor, a heat exchanger for heat recovery and a blower.

Specifically, ethyl acetate and ethanol, employed as solvents in printing processes, are typical VOCs released by the manufacture of packaging. The purification of an air stream containing those compounds is taken as the base case for this study.

The aim of this contribution is to analyze, by means of mathematical simulation, the behavior of the adsorption/desorption system with the purpose of sizing the adsorbent bed and choosing suitable operating conditions. The study is focused on the

* Corresponding author. Departamento de Ingeniería Química, Facultad de Ingeniería, Universidad Nacional de La Plata (UNLP) 1 y 47, CP 1900 La Plata, Argentina.
E-mail address: osvaldommartinez@gmail.com (O.M. Martínez).

http://dx.doi.org/10.1016/j.jenvman.2015.02.028
0301-4797/

Nomenclature

a_v	external surface-area per unit volume of adsorbent, m^{-1}
c_p	volume-specific heat, J m^{-3} K^{-1}
C	molar concentration, mol m^{-3}
d_h	hydraulic diameter, m
d_p	pellet diameter, m
D	rotor diameter, m
D_e	effective diffusivity, m^2 s^{-1}
f	Fanning friction factor
f_{MTZ}	fraction of bed volume corresponding to the mass transfer zone
F_c	concentration factor
h_t	heat transfer coefficient between air stream and adsorbent surface, J m^{-2} s^{-1} K^{-1}
k_m	mass transfer coefficient between air stream and adsorbent surface, m s^{-1}
K	adsorption constant, m^3 mol^{-1}
L	fixed-bed or monolith length, m
L_c	side length of square channel in the monolith, m
ℓ_e	effective diffusion length in the solid (characteristic length), m
N	rotor speed (cycles per hour), h^{-1}
n_c	number of channels per unit cross-section area, m^{-2}
q	number of moles adsorbed per unit volume of adsorbent, mol m^{-3}
Q	saturation concentration (moles per unit volume of adsorbent), mol m^{-3}
r_{pore}	mean pore radius, m
R	universal gas constant, J K^{-1} mol^{-1}
Re	Reynolds number
S	rotor cross-section area, m^2
S_g	specific internal surface-area of adsorbent, m^2 kg^{-1}
Sh	Sherwood number
t	time, s
t_A	adsorption time, s
t_D	desorption time, s
T	absolute temperature, K
u	interstitial velocity, m s^{-1}
V	total volume of adsorbent material, m^3
W_A	mass flow rate of adsorption stream, kg s^{-1}
W_D	mass flow rate of desorption stream, kg s^{-1}
$W_{D,min}$	minimum feasible value of W_D, kg s^{-1}
$W_{D,min}^{ideal}$	minimum feasible value of W_D without transport resistances, kg s^{-1}
z	spatial coordinate inside the adsorbent material, m
Z	axial coordinate in the bed, m

Greek letters

β	parameter in Eq. (2)
ΔH	heat of adsorption, J mol^{-1}
ε_L	void fraction in packed-bed or in the monolith
ε_p	void fraction in adsorbent
λ_{ax}	overall axial effective conductivity, J m^{-1} s^{-1} K^{-1}
λ_p	effective thermal conductivity of adsorbent, J m^{-1} s^{-1} K^{-1}
ρ_{ap}	apparent density of the solid, kg m^{-3}
τ	tortuosity factor
σ	monolith wall-thickness, m

Subscripts

A	adsorption stage/stream
D	desorption stage/stream
g	bulk of the gas stream
i	identification of species, i = 1 (ethyl acetate), i = 2 (ethanol)
macro	macroporous
p	adsorbent material
s	external surface of adsorbent

desorption flow rate, W_D, which determines the VOC concentration in the stream fed to the catalytic incinerator. Then, W_D should be as low as possible in order to increase VOC concentration. The effect of the desorption-stream temperature (T_D) and the amount of adsorbent on W_D is specifically investigated.

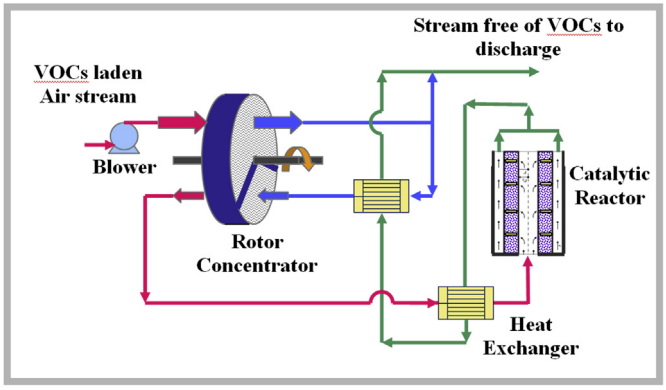

Fig. 1. Simplified flow-sheet for catalytic incineration combined with a rotor concentrator.

2. Definition of the case study

The characteristics of the VOC-laden air stream considered in this study are presented in Table 1. Emission of oxygenated hydrocarbons can bring severe consequences for the environment in the short and long terms. It is then necessary to decrease the VOC concentrations to tolerable levels. According to the *European Commission* (http://ec.europa.eu/environment/air/pollutants/stationary/solvents/legislation.htm), a tolerance of 20 mg/Nm^3 of VOCs (about 5 ppm, in molar basis) in the stream discharged into the atmosphere was considered for calculations. This value corresponds to a time-weighted average, since variations of VOC concentration in the discharge stream are possible, according to the type of treatment employed.

Table 1
Characteristics of the VOC-laden air stream.

Variable	Units	Value
Mass flow rate[a]	kg/s	12.7
Ethyl acetate	Mole fraction	6.23×10^{-4}
Ethanol	Mole fraction	2.55×10^{-4}
Pressure	atm	1
Temperature	°C	50

[a] Permanent emission.

Adsorption/desorption systems lead to a "periodic" type of operation, with an adsorption stage to retain the contaminants in the bed and a desorption stage to restore the initial bed condition. Considering the combined system illustrated in Fig. 1, it is possible to use the heat released by the oxidation reactions to preheat the stream used for the desorption stage. Therefore, the *Temperature Swing Adsorption* (TSA) technique (Ghoshal and Manjare, 2002), has been considered in this study. This option allows reaching an energetically self-sustainable process.

2.1. Adsorbent material and VOC adsorption parameters

Several studies for VOC adsorption, using different types of adsorbents such as activated carbons (Gales et al., 2000, 2003; Águeda et al., 2011; Yamaguchi et al., 2013; Tefera et al., 2014), zeolites (Grande et al., 2006; Yamauchi et al., 2007; Yang et al., 2012) or polymeric adsorbents (Long et al., 2013) have been reported in the literature. Gales et al. (2000, 2003) showed that ethanol and ethyl acetate can be conveniently adsorbed on activated carbon. Given the low cost of activated carbons, this material was chosen to carry out the present analysis.

Values of porosity (ε_p), macro-porosity ($\varepsilon_{p,\ macro}$), specific surface area corresponding to macropores ($S_{g,macro}$) and apparent density (ρ_{ap}) of the activated carbon employed by Gales et al. (2000) are presented in Table 2. From these properties, the average pore radius (r_{pore}) is evaluated by means of the parallel pore model (Table 2). Estimated values of tortuosity, volumetric heat capacity and thermal conductivity (from Gurgel and Grenier, 1990; Gurgel et al., 2005) are also listed in Table 2.

Activated carbons usually present macro and micro porosities, as reported by Gales et al. (2000, 2003). It is generally accepted that micropores are short enough so that surface diffusion can bring nearly equilibrium conditions between the adsorbed phase and the gas phase in the surrounding macropores (Ruthven, 1984). To describe this relationship, the extended Langmuir isotherm for a two-component system was adopted (Eq. (1)), (ethyl acetate: 1 − ethanol: 2):

$$q_i(C_i, T) = \frac{Q_i\ K_i(T)\ C_i}{1 + \sum_{j=1}^{2} K_j(T)\ C_j} \quad i = 1, 2 \tag{1}$$

where Q_i is the saturation concentration (moles of species i per unit volume of adsorbent) and K_i is the adsorption constant for species i, which according to Gales et al. (2003) can be expressed as:

Table 2
Properties of activated carbon and parameters (Q, β, ΔH) of adsorption-isotherms of ethyl acetate and ethanol.

Material or substance	Property or parameter	Units	Value
Activated carbon	ε_p	–	0.70
	$\varepsilon_{p,macro}$	–	0.31
	τ	–	1.50
	$S_{g,macro}$	m^2/kg	53.1×10^3
	ρ_{ap}	kg/m^3	750
	$r_{pore} = 2\ \varepsilon_{p,macro}/(S_{g,macro}\ \rho_{ap})$	nm	16
	λ_p	W/m K	0.76
	$c_{p,p}$	kJ/m^3 K	487
Ethyl acetate	Q	mol/m^3	3.52×10^3
	β	$m^3/K^{3/2}$ mol	2.48×10^{-7}
	(−ΔH)	J/mol	19,600
Ethanol	Q	mol/m^3	4.94×10^3
	β	$m^3/K^{3/2}$ mol	1.47×10^{-10}
	(−ΔH)	J/mol	42,100

$$K_i = \beta_i T^{3/2} \exp(-\Delta H_i/RT) \quad i = 1, 2 \tag{2}$$

Values of Q_i, β_i and ΔH_i from Gales et al. (2000, 2003) are displayed in Table 2.

On the other hand, it is assumed that mass transport from the external surface of the adsorbent takes place through macropores, following a mixed molecular/Knudsen mechanism described by the Bosanquet's expression. As ethyl acetate and ethanol are highly diluted, the molecular diffusivity of each species in air was considered. For the properties of the activated carbon presented in Table 2, the following effective diffusivities were evaluated at T = 50 °C and used throughout the calculations:

$$D_{e,1} = 4.75 \times 10^{-7}\ m^2/s$$

$$D_{e,2} = 6.57 \times 10^{-7}\ m^2/s$$

Gales et al. (2003) measured effective diffusivities of ethyl acetate and ethanol in the activated carbon with properties summarized in Table 2. At 50 C° the reported values are $D_{e,1} = 3.1 \times 10^{-7}$ m^2/s, $D_{e,2} = 4.4 \times 10^{-7}$ m^2/s, which are similar to the values estimated by using Bosanquet's expression.

2.2. Regeneration temperature

In order to choose an appropriate temperature for the desorption stage, as regards the activated-carbon stability, thermogravimetric tests on an activated carbon sample were performed to estimate the consumption of carbon by oxidation when exposed to a temperature of 200 °C in an air stream. It was evaluated that about 11% of the material is lost each year. On the other hand, the conclusion from the study of Yates et al. (2000) performed on a number of activated carbons was that the samples remained at stable conditions up to temperatures of 300 °C. Assuming a conservative criterion, in this study we restrict the analysis to a maximum desorption temperature of 200 °C, while the lowest limit of interest was fixed at 150 °C.

2.3. Adsorption/desorption system

The selection of the adsorption-desorption system requires the definition of two aspects.

On one hand, the layout of the adsorbent material must be chosen. The traditional alternative, involving low investment costs, employs adsorbent pellets packed in a fixed bed (Ramalingam et al., 2012; Yamaguchi et al., 2013; Tefera et al., 2014). During the last decades, techniques have been developed to employ monolithic structures, either totally made of the adsorbent material (Crittenden et al., 2005) or with such material deposited on a supporting matrix (Grande et al., 2006; Moreno-Castilla and Pérez-Cadenas, 2010). The advantages of using a monolithic system have been pointed out in the literature, but the final decision should be taken on economic grounds. A comparison has been undertaken to disclose if clear-cut benefits arise from the use of a monolithic structure. The results are discussed in Section 4.1.

The second aspect concerns the configuration of the adsorption/desorption system. One option is using two beds operating alternatively in adsorption and desorption stages. This configuration has been widely applied to recuperate VOCs from air streams, either using the adsorbent as packed pellets (Ko et al., 2002; Nastaj et al., 2006) or as monolithic structure (Rezaei and Webley, 2010). The second alternative is to arrange the adsorbing material in a rotor concentrator (Yamauchi et al., 2007; Shiraishi et al., 2007; Yang

et al., 2012). This configuration has been generally used with the monolithic adsorbers and frequently in combined systems (Shiraishi et al., 2007; Yang et al., 2012), as presented in Fig. 1. Further discussion about the choice of the configuration will be undertaken in Section 4.2.

3. Modeling and solution methods

The model used for the simulation of the adiabatic adsorption/desorption system presents some simplifying assumptions (Campesi, 2012). Plug flow was assumed for the packed bed adsorber (uniform concentration and temperature in the bed cross-section), uniform distribution of the gas flow into the channels of the monolith was assumed, no axial dispersion/conduction effect was considered, and mass and energy accumulation in the gas stream and inside the macropores of the adsorbent were neglected.

The formulation presented below is suitable either for a packed or for a structured adsorbent. Conservation equations for VOCs (ethyl acetate: 1 and ethanol: 2) and energy in the gas stream are:

$$u\frac{\partial C_{g,i}}{\partial Z}+\frac{(1-\varepsilon_L)}{\varepsilon_L}a_v\,k_{m,i}(C_{g,i}-C_{s,i})=0\quad i=1,2 \tag{3}$$

$$c_{p,g}\,u\frac{\partial T_g}{\partial Z}+\frac{(1-\varepsilon_L)}{\varepsilon_L}a_v\,h_t(T_g-T_p)=0 \tag{4}$$

Conservation equations for VOCs inside the adsorbent material are

$$D_{e,i}\frac{\partial\left(z^{\psi}\partial C_i/\partial z\right)}{z^{\psi}\partial z}-\frac{\partial q_i(C_1,C_2,T)}{\partial t}=0\quad i=1,2 \tag{5}$$

In Eq. (5), $\psi=2$ was taken for the packed bed, assuming nearly spherical pellets, and $\psi=0$ was taken for the monolithic adsorber, assuming that the wall thickness is much smaller than the channel size. Boundary conditions for Eq. (5) are:

$$D_{e,i}\frac{\partial C_i}{\partial z}=k_{m,i}(C_{g,i}-C_{s,i}),\ \text{at}\ z=\ell\quad(i=1,2); \tag{6}$$

$$\frac{\partial C_i}{\partial z}=0,\ \text{at}\ z=0\quad(i=1,2) \tag{7}$$

In Eq. (6) ℓ is the pellet radius for the packed bed and $\ell=\ell_e$: the ratio between the volume of adsorbent and the internal area of the channels for the monolithic adsorber.

Temperature inside the adsorbent material was regarded as being uniform. Then, the following energy conservation equation was employed

$$c_{p,p}\frac{\partial T_p}{\partial t}=\sum_{i=1}^{2}(-\Delta H_i)\frac{\partial\overline{q}_i}{\partial t}+a_v\,h_t(T_g-T_p) \tag{8}$$

In Eq. (8) $\overline{q}_i$ is the average value of q_i on the adsorbent volume.

As regards the mass transfer coefficient k_m in the monolithic adsorber, it was assumed that modules of 20–30 cm in length are employed. It has been checked that this length allows disregarding entrance effects. Then, the asymptotic Sherwood number $Sh=2.977$ for laminar flow in a square channel has been employed to estimate k_m. The expression proposed by Gunn (1978) was used for estimating the Sherwood number in the packed bed adsorber. The heat transfer coefficient h_t was evaluated by considering the similarity with the mass transfer process.

Concerning thermal conduction within the activated carbon, it was checked that temperature remains virtually uniform inside the pellet of the packed bed or along the effective thickness ℓ_e of the monolith.

The validity of neglecting axial thermal conduction in the monolithic adsorber was assessed by comparing this effect with the thermal dispersion effect caused by the external thermal resistance. According to Vortmeyer and Schaefer (1974) an overall axial effective conductivity λ_{ax} (based on the overall cross-section) can be evaluated as

$$\lambda_{ax}=(1-\varepsilon_L)\lambda_p+\left(\varepsilon_L\,u\,c_{p,g}\right)^2/[(1-\varepsilon_L)a_v\,h_t] \tag{9}$$

Alternatively, an effective heat transfer coefficient $h_{t,eff}$ can be defined from (9) as

$$1/h_{t,eff}=1/h_t+a_v\,\lambda_p\left[(1-\varepsilon_L)/\left(\varepsilon_L\,u\,c_{p,g}\right)\right]^2 \tag{10}$$

Eq. (10) is analogous to the approximation presented by Ruthven (1984), Chap. 8, for the mass dispersion problem.

For conditions employed in this work (Section 4), thermal dispersion caused by a finite heat transfer rate, i.e. the second term on the right hand side of (9), was larger than the axial conduction term, except when the desorption step is conducted at a feed temperature of 200 °C, for which both terms are similar, in account of a small flow rate needed to clean the bed (Sections 4.3, 4.5). Even in these cases, calculations made with either $h_{t,eff}$ or h_t showed very slight differences in the temperature axial profile. For the present problem thermal waves are faster than concentration waves. Therefore, the latter waves control the end of either the adsorption or desorption stages, and thermal dispersion has virtually no effect on the relevant features of the process (Section 4). All these facts allow concluding that axial conduction can be safely ignored.

To solve the conservation Eqs. (5)–(7) in the adsorbent material, the *Orthogonal Collocation Method* was employed for discretization along the z-coordinate. Preliminary tests showed that the results using two collocation points were practically undistinguishable from those using additional points (Campesi, 2012). The conservation equations in the fluid were discretized according to the procedure proposed by Matros and Bunimovich (1995).

4. Results

4.1. Comparison between packed-bed and monolithic adsorbers. Discussion of the overall behavior of the adsorption stage

Simulations of both packed-bed and monolith adsorbers were carried out for operating conditions in Table 1 and activated-carbon properties in Table 2. The adsorption stage was simulated with an initially clean bed at 150 °C.

The geometric characteristics of the beds were defined according to the following criteria. Commercial cordierite monoliths have been taken as a reference to choose the basic geometric properties of the monolithic adsorber. To improve mass transfer rates to the walls, a maximum channel density (n_c) for a square-channel monolith and the corresponding wall thickness (σ) from the data

Table 3
Geometric properties of the square monolithic structure.

Property	Units	Value
n_c	channels/m^2	2.48×10^{6}
σ	m	90.8×10^{-6}
R_c	m	0
$L_c=(1/n_c)^{1/2}$	m	6.35×10^{-4}
$\varepsilon_L=(1-\sigma/L_c)^2$	–	0.735
$a_v=4(1-\sigma/L_c)/[L_c(1-\varepsilon_L)]$	m^2_{ads}/m^3_{ads}	20.33×10^{3}
$d_h=L_c-\sigma$	m	5.44×10^{-4}
$\ell_e=1/a_v$	m	4.92×10^{-5}

presented by Boger et al. (2004) were chosen (Table 3). Besides, possible rounding of the channel corners was disregarded. Some other geometric properties, derived from the chosen values of n_c and σ, are also listed in Table 3: channel side L_c, specific area a_v, porosity ε_L, hydraulic diameter d_h, and effective diffusion length in the solid (also known as characteristic length) ℓ_e.

Preliminary evaluations were made by considering that activated carbon was deposited on an inert matrix and the thickness of the composite structure maintained at the value σ given in Table 3. It was concluded (Campesi, 2012) that the adsorbing efficiency of the adsorber is significantly improved if the whole structure is made of adsorbent material. In this way, a larger amount of absorbent material is allowed, which can be effectively utilized because the mass transfer resistance inside the porous adsorbent is almost negligible, as will be discussed later in this paragraph.

For a consistent comparison between the monolith and packed-bed adsorbers, similar values of pressure drop and adsorption time t_A were adopted in both systems. The Ergun equation was used to estimate pressure drop in the packed-bed adsorber and the Fanning equation with (f Re) = 14.2, for laminar flow in a square channel, was used for the monolithic adsorber. An average pressure of 1 atm was assumed.

For a monolith of 2.36 m in length and a cross-section area of 2.86 m^2, the average emission of VOCs reached the tolerable value of 5 ppm at t_A = 840 s. The resulting amount of activated carbon was 1240 kg and the pressure drop through the channels was 0.25 atm.

The cross-section of the packed-bed adsorber was restrained to 10 m^2 (larger values may be unacceptable as regards the cost of vessel heads and difficulties in achieving a uniform flow distribution). The bed length was 0.6 m and the pellet diameter needed to keep the same pressure drop as in the monolith was 1 mm. At these conditions, the operation time was t_A = 808 s, only slightly shorter than for the monolith operation. The geometric features of the packed bed are summarized in Table 4. The resulting mass of activated carbon was 2700 kg, which nearly doubles the amount required in the monolithic adsorber. The main reason for this difference is the requirement of similar pressure drops, which prevents the pellet-size in the packed bed from being reduced. Consequently, the characteristic length ℓ_e in the packed bed is about 3 times larger than in the monolith (Tables 3 and 4), which introduces significantly higher mass transfer resistances in the adsorbent material.

The effect of mass transfer resistances is illustrated in Fig. 2, where concentration ($C_{g,i}$) profiles of ethyl acetate and ethanol in the gas stream and average values inside the adsorbent pores are plotted at the end of the adsorption stage. It should be noted that at this time both beds have reached the temperature of the inlet stream (50 °C), as the thermal waves are fast (the thermal wave in the fixed bed, slower than in the monolith, already reaches the end of the bed at about 150 s). It can be clearly appreciated in Fig. 2 that there are very significant differences between VOC concentrations outside and inside the adsorbent pellet in the packed bed. In turn, internal resistances are considerable higher than film resistances (this effect is not discriminated in Fig. 2).

Table 4
Geometric features of the packed bed.

Property	Units	Value
ε_L	–	0.4
d_p	m	1×10^{-3}
$a_v = 6/d_p$	m^2_{ads}/m^3_{ads}	6×10^3
$d_h = 4\ d_p\ \varepsilon_L/[6\ (1 - \varepsilon_L)]$	m	4.44×10^{-4}
$\ell_e = 1/a_v$	m	1.67×10^{-4}

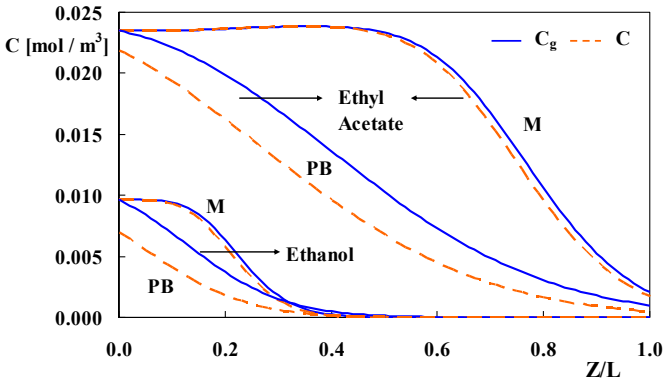

Fig. 2. Concentration profiles in the gas stream and inside the adsorbent pores (average values) of the monolithic (M) and the packed-bed (PB) adsorbers at the end of the adsorption stage ($t_{A,M}$ = 840 s, $t_{A,PB}$ = 808 s). Initial conditions: clean bed at 150 °C.

Although Fig. 2 suggests very low mass transfer resistances in the monolithic adsorber, they still produce a significant degree of dispersion. To appreciate this effect, it is considered the case when adsorption and thermal equilibria between the stream and the adsorbent hold at any bed cross-section. This case will be referred to as *ideal case*. The Method of Characteristics, following Rhee et al. (2001), was employed to evaluate the temperature and concentration patterns in the ideal case. Accordingly, shock waves arise for the displacement of ethanol and ethyl acetate, as shown in Fig. 3 for the monolithic adsorber. The velocity of each of these waves is constant and is very similar to the velocity of the middle point concentration in the corresponding dispersed wave, but the degree of mass dispersion around the middle point is quite significant (Fig. 3).

It is recalled that the length of the bed that remains active at a given time (i.e. the part of the bed that is neither saturated nor clean) is termed Mass Transfer Zone (MTZ). The extent of the MTZ for ethyl acetate at t_A is nearly 50% of the total bed length. The existence of the MTZ accelerates the adsorbate breakthrough and leaves a fraction of the adsorbent without being utilized at the maximum (saturation) level, as discussed e.g. by Miller (1990). In the example, the exit concentration of ethyl acetate reaches the tolerable limit 250 s earlier than the sharp front in the ideal case. In other terms, a larger amount of adsorbent is needed due to mass transfer resistances when t_A is fixed. Also, an adsorber with a shorter MTZ will be able to cope more easily with changes (e.g. composition, flow rates, temperature) in the feed stream.

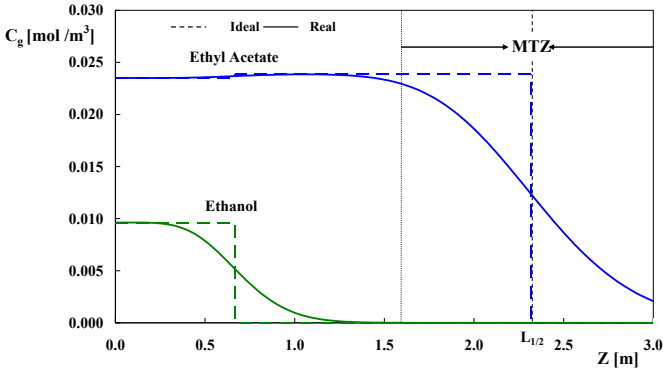

Fig. 3. Ethyl acetate and ethanol concentration profiles at 840 s during the adsorption stage in the monolithic adsorber. Broken lines correspond to shock waves evaluated by ignoring transport resistances. Initial conditions: clean bed at 150 °C.

For the packed bed adsorber, the extent of the MTZ is 100% (Fig. 2), a feature that alternatively explains the inefficiency of the packed-bed.

The overall conclusion from the comparison of monolithic and packed bed adsorbers is that the former provides significant operating advantages. Hence, the monolithic adsorber has been retained for further analysis.

Before ending this section, some other operating features are worth mentioning. In Fig. 2, the concentration of ethyl acetate in the packed bed at the bed exit and at t_A is lower than in the monolith. This is because the tolerance is defined on an average basis and the packed bed allowed for an earlier breakthrough of ethyl acetate. Also, it can be appreciated in Figs. 2 and 3 that ethanol is retained by the adsorbent more strongly than ethyl acetate and therefore the latter always determines the switching time t_A.

4.2. Rotor concentrator

Having shown that the monolithic adsorber performs significantly better than the packed bed, its configuration (Section 2.3) has now to be chosen.

Some advantages of rotor adsorbers over alternating 2-bed adsorbers can be described as follows: simplification of piping and flow-control devices for conveying adsorption and desorption streams, as circulation presents always a single direction; cross-section areas corresponding to adsorption and desorption stages can be different, a fact that allows for pressure drop minimization.

On the other hand, rotor concentrators need a mechanical system for rotation and seals between mobile and static parts.

According to our analysis, a key feature of rotor concentrators is that the discharge streams, specifically that from the desorption stage, show constant values of composition and temperature. This fact maximizes the benefit of using a concentrator, as minimum sizes of heat exchangers and catalyst bed arise when the process stream shows constant properties, in particular VOCs concentration that determines the thermal levels in the heat exchangers and catalytic bed. Therefore, the rotor adsorption system has been chosen to complete our analysis. Monolith geometric features given in Table 3 will be maintained.

It is important to stress that the rotor adsorber can be simulated in a similar way to that of the alternating two-bed system if conductive heat transfer in the angular direction can be neglected. Angular conduction convey heat from the desorption zone to the adsorption zone of the rotor, but the average transfer length for this process is much larger than the heat transfer length from the walls to the flowing stream in the channels. Therefore, the formulation in Section 3 will apply at least to a first order of approximation.

As mentioned above, the rotor cross-section areas for adsorption (S_A) and desorption (S_D) do not necessarily have to be the same. For the case studied, it has been checked that the ratio S_A/S_D has no significant effect on the adsorption/desorption process if it is larger than 1 (Campesi, 2012). Therefore, the ratio S_A/S_D can be used to minimize the total pressure drop. Assuming laminar flow (the usual regime in standard monolithic structures) in the channels, pressure drop is minimized when $(S_D/S_A)^2 = (W_D T_D)/(W_A T_A)$ (Campesi, 2012). As an example, for $W_A/W_D = 3.7$ and $T_D = 150\ ^\circ C$, the optimal ratio becomes $S_A/S_D = 1.7$.

4.3. Evaluation of the adsorption/desorption cycle. Minimum desorption flow rate

To perform the simulation of adsorption/desorption cycles, it is necessary to define conditions of the adsorption and desorption streams (concentration, flow rate, temperature and pressure) and all geometric features of the monolithic bed. Here, the adsorption stream is that defined in Table 1, except for an overpressure necessary for circulation through the different process units (Fig. 1) before the discharge to the atmosphere. An absolute pressure of 1.3 atm at the inlet of the adsorption stage was estimated for that purpose. The desorption stream, a fraction of the clean effluent from the adsorption stage (see Fig. 1), could be considered also at 1.3 atm for the calculations presented here, as most of the overall pressure drop is imposed by the catalytic fixed bed incinerator (Campesi, 2012). Two levels of the desorption-stream temperature T_D have been considered: 150 and 200 °C. For the present calculations the ratio S_A/S_D has been left fixed at 1.7, i.e. the optimal value for $T_D = 150\ ^\circ C$ and $W_A/W_D = 3.7$.

Basically, the calculations should allow defining the switching time t_A of the adsorption stage to obtain a stationary cyclic operation with an average VOC concentration of 5 ppm at the exit of the adsorption stage. To this end, an iterative procedure based on simulating a sequence of adsorption/desorption steps from an initially clean bed at T_D has been employed. Each adsorption step is simulated until the tolerable VOC concentration is reached at a certain switching value t_A. Simulation of a desorption step follows with initial bed conditions as left at the end of the former adsorption step, and it is stopped when $t_D = t_A(S_D/S_A)$ is reached. In this way, the sequence of simulated adsorption steps involves decreasing t_A, as the sequence of desorption steps involves in turn increasing amounts of residual VOCs. This increase becomes eventually negligible (at least if the desorption flow rate is high enough), and consequently the cycles become virtually stationary. At these conditions, the procedure is stopped and the features of the stationary cycle are recorded. In particular, the stationary switching time t_A (and, hence, t_D) thus resulting can in practice be established by setting the rotor speed: $N = S_A/[t_A(S_A + S_D)]$.

The sequence followed by the cycle period, $t_{cycle} = t_A + t_D$ is illustrated in Fig. 4. At the two highest desorption flow rates ($W_D = 3.69$ and 3.82 kg/s) the procedure clearly converges to a stationary cycle. However, at $W_D = 3.56$ kg/s the procedure failed to converge, showing that this value of W_D is less than a minimum value needed for a feasible operation at the tolerable value of VOC exit concentration. This minimum, denoted $W_{D,min}$, is most relevant for the present purpose of using an adsorption/desorption process, as it quantifies the maximum achievable degree of VOC concentration for the chosen operating conditions. Although the exact evaluation of $W_{D,min}$ is rather cumbersome, it can be estimated within an interval narrow enough for any practical purpose. In the example given in Fig. 4, $W_{D,min} \approx 3.69$ kg/s. For a given volume V, the stationary cycle obtained at $W_{D,min}$ will be denoted *SC@$W_{D,min}$*.

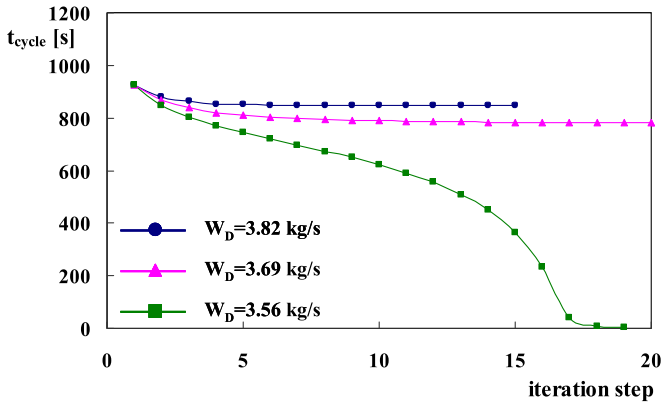

Fig. 4. Variation of the adsorption/desorption period ($t_{cycle} = t_A + t_D$) in the course of iterations, for different values of W_D (D = 4 m, L = 0.5 m, $T_D = 150\ ^\circ C$).

4.4. Evaluation of the adsorbent bed size

The effect of the total adsorbent volume (V) on $W_{D,min}$ has been evaluated in order to make a decision about the size of the adsorber. For this analysis, the geometric features in Table 3 were retained, the diameter of the rotor was kept at D = 4 m and its length L was varied. The results are presented in Fig. 5 for two levels of T_D.

Also drawn in Fig. 5 are the values $W^{ideal}_{D,min}$ corresponding to the minimum desorption flow rate in the ideal case without heat and mass transfer resistances. $W^{ideal}_{D,min}$ depends on T_D, but not on V ($W^{ideal}_{D,min}$=2.79 kg/s, 1.64 kg/s at T_D = 150 °C, 200 °C, respectively). Fig. 5 shows that $W_{D,min}$ decreases as V increases and slowly approaches $W^{ideal}_{D,min}$.

On the other hand, it should be remarked that $W_{D,min}$ increases rapidly in the lower range of V, say for values of V lower than the data point at 1.67 m^3 in Fig. 5. In this lower range, the behavior of adsorption/desorption system – in particular, the value of $W_{D,min}$ – will be significantly affected by any disturbance in the variables defining the stream to be treated. The conclusion reached is that V must be chosen at an intermediate level, such that possible limitations at low V and large adsorbent investment -that will not bring any significant reduction of $W_{D,min}$- can be avoided. For the data in Fig. 5, $W_{D,min}$ only decreases by less than 5% when V is increased from 3.34 to 6.67 m^3. Then, a reasonable range can be defined as 1.7 < V < 3.4 m^3. In this range, values of $W_{D,min}$ remain approximately within 1.15–1.35 $W^{ideal}_{D,min}$.

In order to rationalize the observations made upon the effect of V, the length of the MTZ has been evaluated as $2(L - L_{1/2})$, for each data point in Fig. 5 at the switching time t_A, where $L_{1/2}$ is the length of the bed at which the concentration of ethyl acetate reaches half the value of the saturation front (see Fig. 3). Then, the bed fraction covered by the MTZ is defined as $f_{MTZ} = 2(L - L_{1/2})/L$. Values of f_{MTZ}, corresponding to the results in Fig. 5, along with values of t_A, **N** and factor F_c (which is defined in Section 4.5.) are given in Table 5.

Considering both sets of results, at 150 and 200 °C, we can appreciate that the range 1.67 < V < 3.34 m^3 encompasses values of f_{MTZ} between 0.40 and 0.70. For this range of f_{MTZ}, the values 1.8 < N < 5 rph in Table 5 are typical of rotor concentrators used in VOC purification (Chang et al., 2003; Yamauchi et al., 2007). Therefore, this range of f_{MTZ} can be adopted to establish a design criterion, as it will be convenient from a conceptual point of view and also can bring practical advantages to alleviate the amount of calculations. Procedures to evaluate the adsorbent volume V based on choosing a given value of f_{MTZ} can shorten most significantly the whole procedure, particularly if approximate results are tolerated. Examples of such procedures are proposed below with the help of some examples.

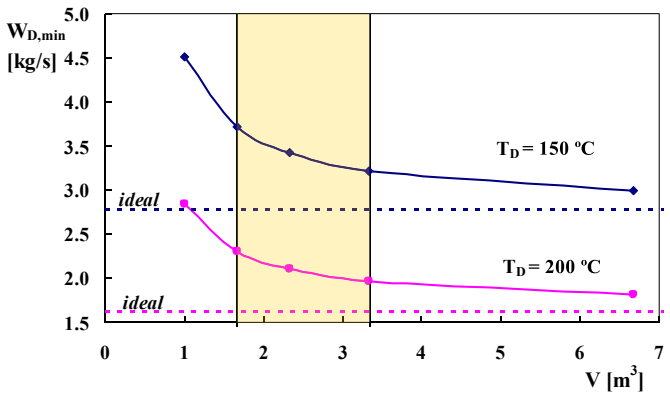

Fig. 5. Variation of $W_{D,min}$ with volume V for two levels of T_D.

Table 5
Operating conditions as a function of the total absorbent volume V.

T_D (°C)	V (m^3)	L (m)	f_{MTZ}	$W_{D,min}$ (kg/s)	F_c	t_A (s)	N (rph)
150	1.00	0.3	0.981	4.51	2.82	223	10.17
	1.67	0.5	0.726	3.71	3.42	480	4.72
	2.34	0.7	0.596	3.42	3.71	748	3.03
	3.34	1.0	0.473	3.22	3.94	1173	1.93
	6.67	2.0	0.283	2.99	4.25	2682	0.84
200	1.00	0.3	0.881	2.84	4.48	257	8.83
	1.67	0.5	0.661	2.30	5.52	518	4.37
	2.34	0.7	0.526	2.11	6.02	807	2.81
	3.34	1.0	0.425	1.97	6.44	1232	1.84
	6.67	2.0	0.255	1.82	6.98	2759	0.82

Assume that employing a desorption stream at T_D = 150 °C, the volume of the adsorbent material is to be calculated for a given value of f_{MTZ}. As a numerical case, f_{MTZ} = 0.447 is chosen. Then, the adsorption stage is first simulated by assuming an initially clean bed and a bed volume V^* is evaluated such that at the end of this adsorption stage the required value of f_{MTZ} is attained. The corresponding volume of the mass transfer zone is $V^*_{MTZ,I} = f_{MTZ}V^*$. With the volume V^*, the evaluation of the *SC@$W_{D,min}$* is performed, as described in Section 4.3, and values of $W^*_{D,min}$, t^*_A and f^*_{MTZ} of such stationary cycle are calculated. For the example, V^* = 2.34 m^3, $W^*_{D,min}$ = 3.42 kg/s, t^*_A = 748 s, f^*_{MTZ} = 0.596 are obtained. The fact that $f^*_{MTZ} > f_{MTZ}$ is due to the effect of the residual amount of ethyl acetate left inside the bed after the stationary desorption step. The volume of the mass transfer zone in the *SC@$W_{D,min}$*, $V^*_{MTZ} = f^*_{MTZ}V^*$, is decomposed as

$$V^*_{MTZ} = V^*_{MTZ,I} + \Delta V^*_{MTZ}$$

where ΔV^*_{MTZ} quantifies the effect of the residual amount of ethyl acetate quoted above. ΔV^*_{MTZ} can thus be evaluated from the known values of V^*_{MTZ} and $V^*_{MTZ,I}$. The size of the bed should be increased from V^* up to a certain value V allowing a closer approach to the desired value f_{MTZ} = 0.447. To this end, it is assumed that the *SC@$W_{D,min}$* with volume V will keep the same effect ΔV^*_{MTZ} evaluated before, but the effect of dispersion in the initially clean bed, $V_{MTZ,I}$, is reckoned to be larger than $V^*_{MTZ,I}$(as V will be larger than V^*). To estimate $V_{MTZ,I}$ we employ the result for the dispersion extent of the front of a single solute subject to a linear adsorption isotherm, which for relatively long beds is proportional to the square root of the bed volume. Thus, $V_{MTZ,I} = V^*_{MTZ,I}(V/V^*)^{1/2}$ is assumed. The volume of the mass transfer zone in the bed of volume V can then be written as $V_{MTZ} = V_{MTZ,I} + \Delta V^*_{MTZ} = V^*_{MTZ,I}(V/V^*)^{1/2} + \Delta V^*_{MTZ}$, which should equal f_{MTZ} V. In this way, the volume V will be estimated from

$$V^*_{MTZ,I}(V/V^*)^{1/2} + \Delta V^*_{MTZ} = f_{MTZ}\,V \qquad (11)$$

Employing the values V^*, $V^*_{MTZ,I}$ and ΔV^*_{MTZ} obtained previously for the desired value f_{MTZ} = 0.447, Eq. (11) allows estimating V = 3.74 m^3, which is only 1.8% less than the true value (V = 3.81 m^3) satisfying f_{MTZ} = 0.447.

This procedure can be followed for any value of f_{MTZ} at the cost of evaluating only one *SC@$W_{D,min}$*. A comparison between the approximation proposed in Eq. (11) and numerical values of V has been carried out for different values of f_{MTZ}, and T_D = 150 and 200 °C. An excellent agreement is found, with a maximum deviation less than 3% in the range 0.40 < f_{MTZ} < 0.70.

To complete the estimation of variables, $W_{D,min}$ and t_A should be evaluated. For t_A, we resort to the observation that the middle-point concentration of the front (recalling comments in Section 4.1 about Fig. 3) travels at constant velocity, and at t_A it is located at

half the MTZ-length from the bed exit. Hence, t_A should be proportional to $V(1 - \frac{1}{2} f_{MTZ})$. Then, having available the set of values (t_A^*, V^*, f_{MTZ}^*), we can write

$$t_A = t_A^* \frac{V\left(1 - \frac{1}{2} f_{MTZ}\right)}{V^*\left(1 - \frac{1}{2} f_{MTZ}^*\right)} \quad (12)$$

It has been checked that Eq. (12) estimate t_A in a highly precise way if the correct value of V is employed. Therefore, the difference in t_A with respect to the true value depends almost exclusively on the accuracy of the estimated value of V.

The following empirical approximation is proposed to estimate $W_{D,min}$ in the range $0.40 < f_{MTZ} < 0.7$, from values $W_{D,min}^*$ and f_{MTZ}^* calculated as explained above:

$$W_{D,min} = W_{D,min}^* \left(f_{MTZ} / f_{MTZ}^*\right) \quad (13)$$

Errors from Eq. (13) are always lower than 10% in the range $0.40 < f_{MTZ} < 0.70$.

The approximate formulation just described, Eqs. (11)–(13), can be viewed as relating a set of values (V^*, f_{MTZ}^*, t_A^*, $W_{D,min}^*$) -and their associated magnitudes $V_{MTZ,I}^*$ and ΔV_{MTZ}^*-, which satisfies a *SC@$W_{D,min}$*, to a set of values (V, f_{MTZ}, t_A, W_{Dmin}) that approximately satisfies a *SC@$W_{D,min}$*. By construction, both sets are linked by the condition $V_{MTZ,I}^* = f_{MTZ} V^*$. Instead, if we remove this condition by choosing a certain reference set (V^*, f_{MTZ}^*, t_A^*, $W_{D,min}^*$), (e.g. by setting V^*), also satisfying a *SC@$W_{D,min}$*, the formulation defined by Eqs. (11)–(13) can be employed to evaluate approximately any other set (V, f_{MTZ}, t_A, $W_{D,min}$) by fixing any of their components (e.g., V). If this approach works correctly, it would be highly convenient for carrying out a parametric study, e.g. by sweeping values of f_{MTZ} or V, just at the cost of evaluating only one *SC@$W_{D,min}$* for the reference set (V^*, f_{MTZ}^*, t_A^*, $W_{D,min}^*$).

The precision of the results employing this additionally simplified procedure will depend in some extent on the choice of the reference set. However, it has been checked that as far as the reference value f_{MTZ}^* lies within the recommended range $0.40 < f_{MTZ} < 0.70$, the values of the set (V, f_{MTZ}, t_A, $W_{D,min}$) will be suitably estimated if f_{MTZ} also lies within the recommended range. In general, within the studied range of temperature T_D, values of V, t_A and W_{Dmin} are estimated with errors less than 10%.

4.5. Significance of attainable values of $W_{D,min}$

Table 5 shows that, for a given value of V, significantly lower values of $W_{D,min}$ can be employed at the higher temperature $T_D = 200$ °C. The ratio $F_c = W_A/W_{D,min}$ is also the maximum feasible ratio of VOC concentration between the actual stream fed to the catalytic incinerator and the waste air stream (Fig. 1). Values of F_c at $T_D = 150$ °C are in general higher than 3 (see Table 5), while those at $T_D = 200$ °C are about 50% larger.

The effect of F_c, in the range of values in Table 5, on the size of the catalytic bed and recuperative heat exchangers was analyzed by Campesi et al. (2012b). It was shown that the catalyst volume and heat exchange areas are approximately reduced at rates $F_c^{-1.7}$ and F_c^{-2}, respectively. Therefore, a substantial advantage is achieved by inclusion of an adsorption/desorption cycle, even when the activated carbon bed is operated at safely low temperatures ($T_D < 200$ °C).

5. Conclusions

With the purpose of reducing the amount of catalyst and surface-area of recuperative heat exchangers required for VOC incineration, thermal swing adsorption on activated carbon has been analyzed as a previous step for VOC concentration. The case of mixtures of ethyl acetate and ethanol carried in effluent air streams from printing processes has been specifically dealt with in this study.

The effect of heat and mass transfer resistances turned out to be conclusive when packed-bed and monolithic adsorbers were compared on the basis of the same pressure drop and adsorption time. Thus, around twice the mass of adsorbing material is required in the packed-bed. The main reason for this result lies in the size of the pellet, which in the packed-bed should be significantly larger than the wall thickness in the monolith.

The monolithic adsorber, set and operated in a rotor, was then chosen to proceed with the analysis. This choice was mainly due to the fact that a rotor allows for an output stream with constant concentration and temperature, a key feature to minimize the size of the catalytic reactor and heat-exchange system. A further advantage of using the rotor concentrator is that total pressure drop can be minimized by choosing suitable fractions of the rotor cross-section for the adsorption and desorption stages.

Simulations of the stationary adsorption/desorption cycles in the rotor concentrator showed that a feasible operation of the concentrator is achieved above a minimum value of W_D, denoted by $W_{D,min}$. This is a desirable level for W_D, as it provides a stream to be processed in the catalytic incinerator with maximum concentration of VOCs. $W_{D,min}$ decreases monotonically with V towards an ideal value $W_{D,min}^{ideal}$, corresponding to an operation without the effect of mass and heat transfer resistances. The lower range of V is not convenient, as it corresponds to the region in which $W_{D,min}$ shows more sensitivity, while the upper range of V involves a large mass of adsorbent without yielding a significant decrease of $W_{D,min}$. The middle range appears as the appropriate one; therefore, a given value of V within this range should be chosen to design the unit. The whole procedure described above to identify a suitable range of V is very tedious and computationally demanding. It is therefore advisable to characterize that range by the corresponding range of mass transfer zone in the adsorption stage, which is given by $0.40 < f_{MTZ} < 0.70$. An operation within this range provides a reasonable degree of utilization of the adsorbent material and enough flexibility for facing changes in the operating conditions or in the adsorption capacity of the activated carbon. The choice of a given value for f_{MTZ} is proposed as a design criterion. It is also shown that an approximate procedure on this basis allows for both the design of the unit and the evaluation of operating conditions with modest computational effort.

Although the conclusions and procedures discussed here will not be of universal application, it is expected that they can be useful for the analysis of similar problems involving VOC laden air streams. Regarding the suggested approximate procedure, it is advisable to test if it can render acceptably precise results for a given multi-component VOC system, in particular when the first eluted component shows a strongly non-linear adsorption isotherm. In any case, we expect that the rationale employed for such an approximation can be employed at least as a basis to develop an *ad-hoc* procedure.

Finally, in the case studied in this work, it was found that the thermal swing adsorption process allows to increase by 3–6 times the VOC concentration in the stream to be catalytically treated, in a range of desorption temperatures from 150 to 200 °C. In a previous contribution, it was shown that such levels of VOC concentration enable substantial savings in the amount of catalyst needed for incineration and in the surface-areas of recuperative heat exchangers.

Acknowledgments

The authors wish to thank the financial support of the following argentine institutions: ANPCyT- MINCyT (PICT'11–1641), CONICET (PIP 0304) and UNLP (PID I177). O. M. Martínez and G. F. Barreto are research members of CONICET and C.D. Luzi holds a grant from CONICET.

References

Águeda, V.I., Crittenden, B.D., Delgado, J.A., Tennisonb, S.R., 2011. Effect of channel geometry, degree of activation, relative humidity and temperature on the performance of binderless activated carbon monoliths in the removal of dichloromethane from air. Sep. Purif. Technol. 78, 154–163.

Boger, T., Heibel, A.K., Sorensen, C.M., 2004. Monolithic catalysts for the chemical industry. Ind. Eng. Chem. Res. 43, 4602–4611.

Campesi, M.A., 2012. Estudio de Sistemas Combinados de Combustión Catalítica de VOCs. Doctoral Dissertation. Universidad Nacional de La Plata, Argentina.

Campesi, M.A., Mariani, N.J., Bressa, S.P., Pramparo, M.C., Barbero, B., Cadús, L., Barreto, G.F., Martínez, O.M., 2012a. Kinetic study of the combustion of ethanol and ethyl acetate mixtures over a MnCu catalyst. Fuel Process. Technol. 103, 84–90.

Campesi, M.A., Luzi, C.D., Martínez, O.M., Barreto, G.F., 2012b. Effect of concentration by thermal swing adsorption on the catalytic incineration of VOCs. Int. J. Chem. React. Eng. 10.

Chang, F.-T., Lin, Y-Ch, Bai, H., Pei, B.-S., 2003. Adsorption and desorption characteristics of semiconductor volatile organic compounds on the thermal swing honeycomb zeolite concentrator. J. Air Waste Manag. Assoc. 53, 1384–1390.

Crittenden, B., Patton, A., Juin, C., Perera, S., Tennison, S., Botas Echevarría, J.A., 2005. Carbon monoliths: a comparison with granular materials. Adsorption 11, 537–541.

Delimaris, D., Ioannides, T., 2009. VOC oxidation over CuO–CeO_2 catalysts prepared by a combustion method. Appl. Catal. B Environ. 89, 295–302.

Everaert, K., Baeyens, J., 2004. Catalytic combustion of volatile organic compounds. J. Hazard. Mater. B109, 113–139.

Gales, L., Mendes, A., Costa, C., 2000. Hysteresis in the cyclic adsorption of acetone, ethanol and ethyl acetate on activated carbon. Carbon 38, 1083–1088.

Gales, L., Mendes, A., Costa, C., 2003. Recovery of acetone, ethyl acetate and ethanol by thermal pressure swing adsorption. Chem. Eng. Sci. 58, 5279–5289.

Ghoshal, A.K., Manjare, S.D., 2002. Selection of appropriate adsorption technique for recovery of VOCs: an analysis. J. Loss Prev. Proc. 15, 413–421.

Grande, C.A., Cavenati, S., Barcia, P., Hammer, J., Fritz, H.G., Rodrigues, A.E., 2006. Adsorption of propane and propylene in zeolite 4A honeycomb monolith. Chem. Eng. Sci. 61, 3053–3067.

Gunn, D.J., 1978. Transfer of heat or mass to particles in fixed and fluidized beds. Int. J. Heat Mass Transf. 21, 467–476.

Gurgel, J.M., Grenier, P.H., 1990. Mesure de la conductivité thermique du charbon actif AC-35 en présence de gaz. Chem. Eng. J. 44, 43–50.

Gurgel, J.M., Tavares, F.R.M., Oliveira, P.A., Marques, A.S., Oliveira, L.G., 2005. Experimental results for thermal conductivity of adsorbed natural gas on activated carbon. In: 17th European Conference on Thermophysical Properties, Bratislava, Slovakia, Paper 231.

Khan, F.I., Goshal, A.Kr, 2000. Removal of volatile organic compounds from polluted air. J. Loss Prev. Proc. 13, 527–545.

Ko, D., Kim, M., Moon, I., Choi, D.-k., 2002. Analysis of purge gas temperature in cyclic TSA process. Chem. Eng. Sci. 57, 179–195.

Long, C., Yu, W., Li, A., 2013. Adsorption of n-hexane vapor by macroporous and hypercrosslinked polymeric resins: equilibrium and breakthrough análisis. Chem. Eng. J. 221, 105–110.

Matros, Y.Sh, Bunimovich, G.A., 1995. Control of volatile organic compounds by the catalytic reverse process. Ind. Eng. Chem. Res. 34, 1630–1640.

Miller, G.Q., 1990. Multiple zone adsorption process. USA Patent, Number 4964888.

Moreno-Castilla, C., Pérez-Cadenas, A.F., 2010. Carbon-based honeycomb monoliths for environmental gas-phase applications. Materials 3, 1203–1227.

Nastaj, J.F., Ambrozek, B., Rudnicka, J., 2006. Simulation studies of a vacuum and temperature swing adsorption process for the removal of VOC from waste air streams. Int. Commun. Heat Mass 33, 80–86.

Nikolajsen, K.M., Kiwi-Minsker, L., Renken, A., 2006. Structured fixed-bed adsorber based on zeolite-sintered metal fibre for low concentration VOC removal. Chem. Eng. Res. Des. 84, 562–568.

Ramalingam, S.G., Pré, P., Giraudet, S., Le Coq, L., Le Cloirec, P., Baudouin, O., Déchelotte, S., 2012. Different families of volatile organic compounds pollution control by microporous carbons in temperature swing adsorption processes. J. Hazard. Mater. 221–222, 242–247.

Rezaei, F., Webley, P., 2010. Structured adsorbents in gas separation processes. Sep. Purif. Technol. 70, 243–256.

Rhee, H., Aris, R., Amundson, N.R., 2001. First-order Partial Differential Equations. In: Theory and Application of Hyperbolic Systems of Quasilinear Equations, vol. 2. Dover Publications, Inc., New York.

Ruthven, D.M., 1984. Principles of Adsorption and Adsorption Processes. John Wiley & Sons, New York.

Santos, V.P., Pereira, M.F.R., Órfão, J.J.M., Figueiredo, J.L., 2011. Mixture effects during the oxidation of toluene, ethyl acetate and ethanol over a cryptomelane catalyst. J. Hazard. Mater. 185, 1236–1240.

Shiraishi, F., Nomura, T., Yamaguchi, S., Ohbuchi, Y., 2007. Rapid removal of trace HCHO from indoor air by an air purifier consisting of a continuous concentrator and photocatalytic reactor and its computer simulation. Chem. Eng. J. 127, 157–165.

Sramek, M., Ditl, P., Neumanová, E., 2004. Gas purification by combined method adsorption-catalytic oxidation. In: Proc. of CHISA 2004-16th Int. Congress of Chem. and Proc. Eng., Praga, Zchec Republic, Paper N# 0580.

Tefera, D.T., Hashisho, Z., Philips, J.H., Anderson, J.E., Nichols, M., 2014. Modeling competitive adsorption of mixtures of volatile organic compounds in a fixed-bed of beaded activated carbon. Environ. Sci. Technol. 48, 5108–5117.

Vortmeyer, D., Schaefer, R.J., 1974. Equivalence of one- and two-phase models for heat transfer processes in packed beds: one dimensional theory. Chem. Eng. Sci. 29, 485–491.

Yamauchi, H., Kodama, A., Hirose, T., Okano, H., Yamada, K., 2007. Performance of VOC abatement by thermal swing honeycomb rotor adsorbers. Ind. Eng. Chem. Res. 46, 4316–4322.

Yamaguchi, T., Aoki, K., Sakurai, M., Kameyama, H., 2013. Development of new hybrid VOCs treatment process using activated carbon and electrically heated alumite catalyst. J. Chem. Eng. Jpn. 46, 802–810.

Yang, R.T., 1997. Gas Separation by Adsorption Processes. Imperial College Press, London.

Yang, J., Chen, Y., Cao, L., Guo, Y., Jia, J., 2012. Development and field-scale optimization of a honeycomb zeolite rotor concentrator/recuperative oxidizer for the abatement of volatile organic carbons from semiconductor industry. Environ. Sci. Technol. 46, 441–446.

Yates, M., Blanco, J., Avila, P., Martin, M.P., 2000. Honeycomb monoliths of activated carbons for effluent gas purification. Micropor. Mesopor. Mat. 37, 201–208.